Biomedical Signal Processing and Control 71 (2022) 103228

Contents lists available at ScienceDirect

Biomedical Signal Processing and Control

journal homepage: www.elsevier.com/locate/bspc

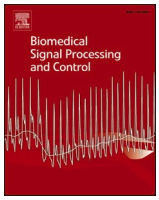

Arrhythmia classification of LSTM autoencoder based on time series anomaly detection

Pengfei Liu, Xiaoming Sun *, Yang Han, Zhishuai He, Weifeng Zhang, Chenxu Wu

Heilongjiang Province Key Laboratory of Laser Spectroscopy Technology and Application, Harbin University of Science and Technology, Harbin 150080, China

ARTICLE INFO

Keywords:
Heartbeat classification
Arrhythmia
Deep learning
LSTM
Autoencoder

ABSTRACT

Electrocardiogram (ECG) is widely used in the diagnosis of heart disease because of its noninvasiveness and simplicity. The time series signals contained in the signal are usually obtained by the professional medical staff and used for the classification of heartbeat diagnosis. Professional physicians can use the electrocardiogram to know whether the patient has serious congenital heart disease and whether there is an abnormal heart structure. A lot of work has been done to achieve automatic classification of arrhythmia types. For example, Autoencoder can obtain the time series characteristics of ECG signals and be used for ECG signal classification. However, some traditional methods are abstruse and difficult to understand in principle. In the classification of arrhythmias carried out in recent years, some researchers only use Autoencoder to provide structural characteristics, without giving too much explanation to the design reasons. Therefore, we optimized a new network layer design based on LSTM to obtain the autoencoder structure. This structure can cooperate with the ECG preprocessing process designed by us to obtain better arrhythmia classification effect. This method enables direct input of ECG signals into the model without complicated preprocessing such as manual parameter input. Also, it eliminates the gradient vanishing problem existing in traditional convolutional neural network. We used five different types of ECG data in MIT-BIH arrhythmia database and MIT-BIH supraventricular arrhythmia database: atrial premature beats (APB), left bundle branch block (LBBB), normal heartbeat (NSR), right bundle branch block (RBBB) and ventricular premature beats (PVC). High accuracy, precision and recall were obtained. Compared with traditional methods, this method has better performance in arrhythmia classification.

1. Introduction

Electrocardiogram (ECG) is a technology that uses an electrocardiograph to record the changes in the electrical activity of the heart during each heartbeat cycle from the body surface. Its main components include QRS composite wave, P wave, T wave and so on. Professional physicians can know whether patients have serious congenital heart disease or cardiac structural abnormalities through ECG [1]. In addition, diseases such as acute myocardial ischemia and myocardial infarction can also be quickly identified by ECG. ECG is an important standard for arrhythmia diagnosis. Arrhythmia disease refers to the problem of fast or slow heartbeat that exceeds the general range, tachycardia, bradycardia, or arrhythmia caused by abnormal cardiac autonomy or conduction disorders. However, the diagnosis of arrhythmia requires a doctor with professional training to visually evaluate many irregular electrocardiograms, which is a very time-consuming and subjective process. Therefore, it is difficult to accurately classify arrhythmia.

In studying the state changes of human system, biomedical engineering can analyze and control these changes by integrating the principles of physics, chemistry, mathematics, computer and engineering. In previous studies, many excellent methods have been proposed [48–52]. Therefore, it is feasible to use computer-aided diagnosis technology to realize computer automatic identification of arrhythmia types. The classification of ECG can be divided into four parts: preprocessing, heartbeat segmentation, feature extraction and classification. There have been several methods proposed for the classification in literature. Some researchers use wavelet transform to extract ECG signal, because conceptually, wavelet transform can extract both time-domain and frequency-domain information of ECG signal [2]. Wavelet transform can decompose the signal into various components and then recombine them into the original signal without losing the main information. This situation is also called synthesis or reconstruction [3]. Mohan Rai et al. extracted the features of the original ECG signals by using discrete wavelet transform, and finally obtained 97.8% of the total accuracy

* Corresponding author.
E-mail address: sunxiaoming@hrbust.edu.cn (X. Sun).

https://doi.org/10.1016/j.bspc.2021.103228
Received 8 July 2021; Received in revised form 23 August 2021; Accepted 30 September 2021
Available online 9 October 2021

through the training of back propagation network (BPN) and feedforward network (FFN) [4]. Convolutional neural network (CNN) is also widely used in the morphological analysis of physiological signals due to its displacement invariance and outstanding capture position characteristics. Rajpurkar et al. built a 34-layer CNN model to detect a total of 64,121 records of arrhythmia data, and finally achieved a total accuracy of 80% [5]. Acharya et al. constructed an 11-layer CNN model to segment ECG signals, and successfully realized the automatic identification of shock and non-shock arrhythmias [6]. There are many other methods proposed by researchers to analyze ECG signals [47], including multi-layer perceptron (MLP) [4], autoregressive modeling [7], self-organizing maps (SOM) [8], long-short-term memory (LSTM) and so on [9].

However, most papers often overlook an important issue when using wavelet transform methods to obtain the representation parameters of the ECG signal. Although the wavelet function is excellent in the application of extracting multi-scale features, its basic principles are not simple. . In contrast, the simplest method is to directly use the numerical points displayed on the ECG curve as the representation parameters. The significant difference between the deep learning-based ECG classification method and the traditional method is that the deep learning method can combine the two steps of ECG signal feature extraction and classification. In other words, the deep learning method can extract and learn useful features from the target signal. As an unsupervised learning algorithm, autoencoder has a very good ability to extract data feature representation. As a type of neural network, the autoencoder can be regarded as composed of two parts: an encoder and a decoder with reconstruction function. The main purpose of this network is to reconstruct its input so that its hidden layer can learn useful features of the input data. And back propagation is applied so that the target value can be set to be the same as the input value [10]. Therefore, the useful features of the data displayed on the ECG curve can be directly extracted by using the automatic encoder.

At present, ECG classification are mainly focused on CNN in addition to using wavelet transform. As for CNN, with the increasing number of stacked neural network layers, its learning ability will gradually increase. However, simply increasing the number of stacked neural network layers does not contribute to the accuracy of the CNN network model. However, with the increasing number of stacked layers, the problem of gradient disappearance in the CNN network model is gradually exposed [11]. Although many methods have been proposed by researchers to solve this thorny problem, such as normalized initialization methods or intermediate normalized methods [12,13], there is still a problem that the model accuracy is reduced due to the increase of network layers. The LSTM network does not have the problem of gradient disappearance, therefore LSTM network can perform better than CNN in most cases. However, LSTM network is rarely used for the classification of arrhythmias.

We design and optimize a new autoencoder structure based on LSTM network layer, which can cooperate with our ECG preprocessing process to obtain better arrhythmia classification effect. Compared with traditional classification method, there was no need to manually input features of the model, and the problem of gradient disappearance was solved. The accuracy of ECG classification can be improved with this simple model.

2. Material and methods

2.1. Database

In this study, the same kind and amount of ECG signals were extracted from MIT-BIH arrhythmia database [14] and MIT-BIH supraventricular arrhythmia database [43] for experiments. The MIT-BIH arrhythmia database contains 48 and a half hours of two-channel Holter ECG excerpts, recorded at a rate of 360 samples per second per channel in the 10 mV range. It is digitized with 11-bit resolution. Two or more cardiologists independently annotate each record to resolve annotation differences and obtain computer-readable reference annotations for each beat attached to the database. Note that the two channels are channel 1 and channel 2. All the details of the database are recorded in Table 1.

Table 1
Lead types and record grouping of MIT-BIH arrhythmia database.

Channel 1	MLII	MLII	MLII	V5	V5	MLII
Channel 2	V2	V4	V5	V2	MLII	V1
Records	103 117	124	100 123	102 104	114	101 105 106 107 108 109 111 112 113 115 116 118 119 121 122 200 201 202 203 205 207 208 209 210 212 213 214 215 217 219 220 221 222 223 228 230 231 232 233 234

The MIT-BIH supraventricular arrhythmia database contains 78 half-hour two channel ECG excerpts. The recorded heartbeat beat type is first automatically calibrated by the Marquette electronics 8000 Holter scanner, and then checked and corrected by professional doctors. In the segmentation of ECG signals, continuous beats were used in the arrhythmia group. The continuous ECG signal beats were divided into single beats. Each heartbeat beat is composed of 300 samples. ECG segmentation is based on the manually marked R-wave peak position record file provided in the database [15]. In order to retain complete heartbeat information, we chose to retain each R-peak position as well as 99 samples before and 200 samples after the R-peak position. Fig. 1 shows five different types of waveforms. Table 2 shows the types of arrhythmias used in this study and the number of random samples.

In this study, 97,300 heartbeats were used in each database for training, testing and verification. 75% of the data were randomly selected as the training set. The rest 25% of the data was randomly assigned to validation set (65%) and test set (35%). The details of the data distribution of the training set, test set, and verification set are shown in Fig. 2.

2.2. Filter out the noise in the signal

Human ECG signal is a very weak physiological low-frequency electrical signal. In most cases, the maximum amplitude does not exceed 5 mV, and the signal frequency is between 0.05 and 100 Hz. The ECG signal is picked up by electrodes installed on the surface of the human skin. Because of polarization between electrode and skin tissue, it will cause serious interference to ECG signal [16]. In addition, power frequency interference is also included in the original ECG signal [17]. In order to effectively remove these noises and preserve the original characteristics of the ECG signal, we designed a low-pass filter [18] and an adaptive filter [19] to filter out the noise.

The frequency of EMG signal is between 20 Hz and 5000 Hz. The frequency of its main components is related to the type of muscle. Generally in the range of 30HZ to 300HZ, and the frequency of the ECG signal is mainly concentrated between 5HZ and 20HZ [20]. So a low pass filter was selected to filter out EMG interference. According to the classification of filter passband characteristics, there are mainly four kinds of classical filters: Butterworth filter, Chebyshev filter, Bessel filter and Elliptic filter. Butterworth filter is famous for its maximum flatness in the passband. So Butterworth function was chosen to approximate the system function of the filter. The calculation formula of its amplitude square function is as follows.

$$|H_a(j\Omega)|^2 = \frac{1}{1+\left(\frac{\Omega}{\Omega_c}\right)^{2N}} \tag{1}$$

where N is the order of the filter and Ω_c is the frequency when the

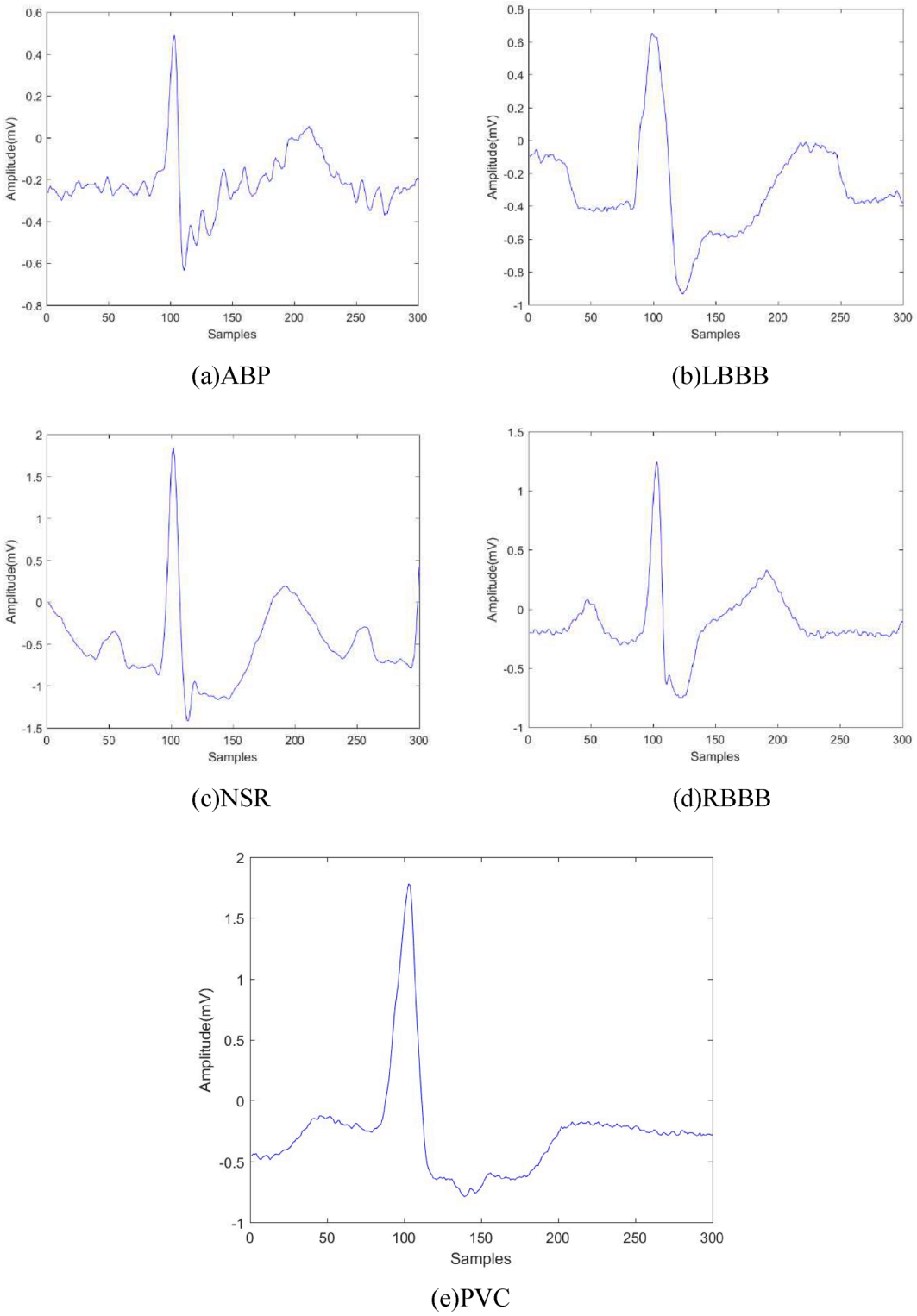

Fig. 1. Five types of heartbeats in MLII lead:(a)ABP,(b)LBBB,(c)NSR,(d)RBBB,(e)PVC.

amplitude drops to -3. It can be seen from Formula (1) that Butterworth filter only needs two parameter representations: N and Ω_c. So the order N of low-pass filter is solved:

$$N = \frac{1}{2}\frac{lg\left(\frac{10^{0.1A_s}-1}{10^{0.1A_p}-1}\right)}{lg\left(\frac{\Omega_s}{\Omega_p}\right)} \tag{2}$$

In formula (2), A_s represents the stopband cutoff frequency of the low-pass filter, which is taken as 100 Hz. A_p is the cut-off frequency of passband, and the value is 80 Hz. Ω_s is stopband attenuation, and the value is 1.6. Ω_p is passband attenuation, with a value of 1.4 [37].

Next, the amplitude function formula of the filter can be obtained from the (1) formula:

Table 2
Arrhythmia types used in the study and the distribution of data.

Arrhythmia Types	Data size(beat)
Atrial Premature Beat (APB)	3000
Left Bundle Branch Block (LBBB)	8000
Normal Sinus Rhythm (NSR)	72,000
Right Bundle Branch Block (RBBB)	7200
Premature Ventricular Contraction (PVC)	7100
Total Beat:	97,300

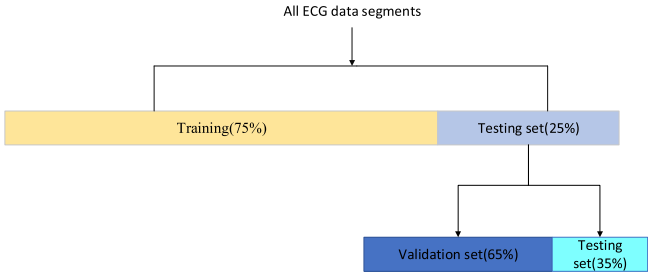

Fig. 2. The data distribution details for training、testing and validation.

$$|H_a(j\Omega)| = \frac{1}{\sqrt{1+(-1)^N\left(\frac{s}{\Omega_c}\right)^{2N}}} \quad ,s = j\Omega,\ \Omega = -\infty \sim +\infty \tag{3}$$

(3)

$$1+(-1)^N\left(\frac{S}{\Omega_c}\right)^{2N} = 0$$

We can solve for s in formula (4) in two ways. When N is even:

$$s = \Omega_c e^{j\frac{(2k+1)}{2N}\pi} \tag{5}$$

Similarly, when N is odd:

$$s = \Omega_c e^{j\frac{k}{N}\pi} \tag{6}$$

After summing up the above formula (5) and formula (6), it can be concluded that:

$$P_k =, \begin{cases} \Omega_c e^{j\frac{2k+1}{2N}\pi} & ,N: even\ number, k = 0,1,2,\cdots 2N-1 \\ \Omega_c e^{j\frac{k}{N}\pi} & ,N: odd\ number, k = 0,1,2,\cdots 2N-1 \end{cases} \tag{7}$$

The solution P_k obtained by the above formula is the pole of the system function. In the complex frequency domain, these points are equidistant on the circle with radius Ω_c. The total number is $2N$ [38]. In order to make the established low pass filter stable, only the point of the pole in the left half plane of the complex frequency domain space can be selected [21]. After the stable pole is selected, the transfer function of the low-pass filter in the analog domain can be obtained as shown in formula (8):

$$H_a(s) = \prod_{Re[p_k]<0} \frac{\Omega_c}{s - p_k} \tag{8}$$

$$s = \frac{2}{T}\frac{1-z^{-1}}{1+z^{-1}} \tag{9}$$

Finally, the s variable in the analog domain transfer function $H_a(s)$ in formula (8) is transformed by formula (9), and finally the digital domain transfer function $H(z)$ is obtained. So far, the design of the low-pass filter has been completed, and the original lead II ECG signal passes through the filter to filter out EMG interference.

In EMG measurement, the interference of power frequency is often represented by the interference of 50 Hz electric field and 50 Hz magnetic field. When the center frequency of power frequency interference has drift, the filtering effect of ordinary filter will be affected to a certain extent, and adaptive filter is very useful for eliminating power frequency interference [22]. Therefore, the basic principles of the LMS algorithm [23] can be used to design an adaptive filter. The schematic diagram of the filter is shown in Fig. 3:

The input D (n) of the Main input channel contains ECG signal and power frequency interference noise. The Reference input includes cross-correlation reference noise. S (n) is a useful component of the Main input channel. Y (n) is the adjusted output through the adaptive filter. The order of the adaptive filter we designed is 2. X1 and X2 respectively correspond to power frequency interference and power frequency interference with a phase shift of 90 degrees. W1 and W2 are weighted coefficients, where W1 corresponds to power frequency interference coefficient and W2 corresponds to power frequency interference coefficient with 90 degree phase shift. The weighted power frequency interference is added and subtracted from the main input channel to eliminate the power frequency interference in the main input channel. Iteratively adjust the weighting coefficient through formulas (10), (11), (12), and (13). The iterative process is [23]:

$$w_1(n+1) = w_1(n) + \mu S(n) X_1(n) \tag{10}$$

$$w_2(n+1) = w_2(n) + \mu S(n) X_2(n) \tag{11}$$

$$Y(n) = X_1(n) w_1(n) + X_2(n) w_2(n) \tag{12}$$

$$S(n) = D(n) - Y(n) \tag{13}$$

In the formula, μ is the convergence factor, and its value is 0.1. The number of iterations is n. By iterating the above formula group continuously, the weighting coefficient is adjusted to obtain the ECG output

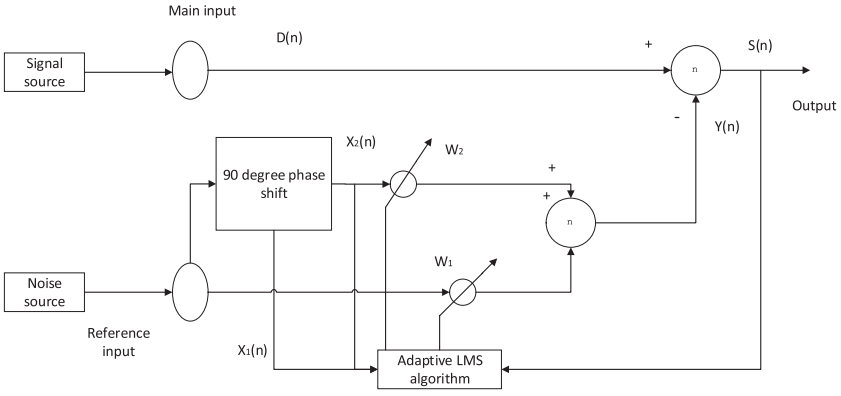

Fig. 3. Schematic diagram of adaptive filter.

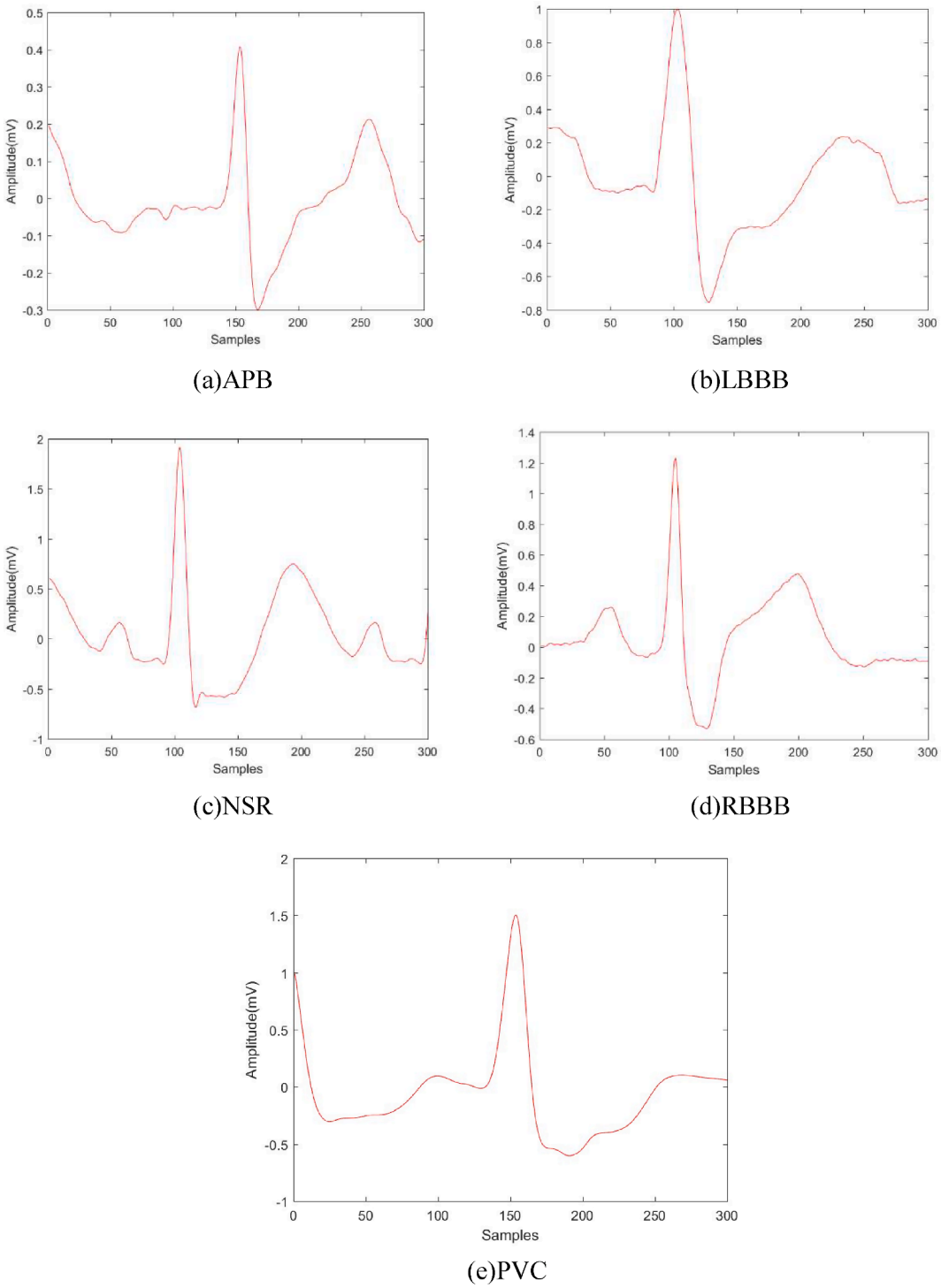

Fig. 4. Five types of heartbeats after filtering in MLII lead:(a)APB,(b)LBBB,(c)NSR,(d)RBBB,(e)PVC.

signal $S(n)$ after eliminating the power frequency interference. So far, the adaptive filter has been designed, and the original lead II ECG signal is filtered by the filter. The waveforms of five different ECG signals after the above filtering steps are shown in Fig. 4. By comparing with the five original input ECG signal waveforms in Fig. 1 above, it can be clearly seen that the noise in the original ECG signal is filtered out.

2.3. Long-short term memory(LSTM)

LSTM is a special RNN network which can deal with long memory problems. Compared with traditional RNN, LSTM has better long-term information memory ability than RNN. LSTM can learn long-term dependence information and avoid the problem of vanishing gradients in conventional RNN networks. All RNNs have a chain form of repeating neural network modules. LSTM contains memory cells, memory blocks and gate units [24]. The gate unit controls the state of memory cells. For example, the amnesia gate controls the LSTM to determine with a certain probability whether to forget the hidden cell state of the next layer. The input gate is responsible for processing input at the current sequence position. Its calculation flow chart is shown in Fig. 5:

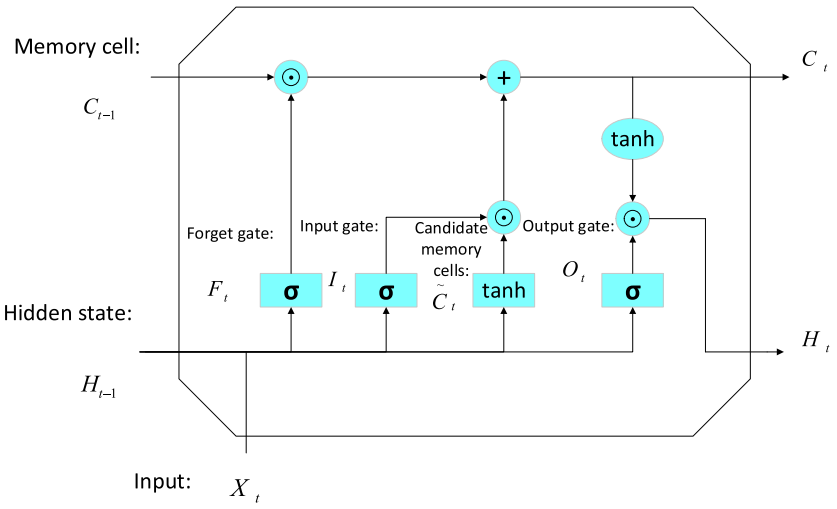

Fig. 5. Calculation flow chart of LSTM.

Where F_t represents the oblivion gate at the current moment t.I_t represents the input gate at the current time t.O_t represents the output gate of the current time t.σ stands for the full connection layer and the activation function. $\odot$stands for Multiplication by Elements. $\tilde{C}_t$ represents the state of candidate memory cells at the current time t.C_t represents the state of memory cells of t at the current time. C_{t-1} represents the state of memory cells in the previous time step. H_t represents the hidden state of the current time t.H_{t-1} represents the hidden state of the previous time step. X_t represents the input of the current time. The gate input of LSTM is the current time step input X_t and the previous time step hidden state H_{t-1}. The output is calculated by the fully connected layer whose activation function is the sigmoid function. Specifically, suppose that the number of hidden units is h, the small batch input $X_t \in R^{n\times d}$ (sample number is n, input number is d) of the given time step t and the hidden state $H_{t-1} \in R^{n\times h}$ of the previous time step. The calculation formulas of input gate $I_t \in R^{n\times h}$, forgetting gate $F_t \in R^{n\times h}$ and output gate $O_t \in R^{n\times h}$ of time step t are as follows[24]:

$$I_t = \sigma(X_t W_{xi} + H_{t-1} W_{hi} + b_i) \tag{14}$$

$$F_t = \sigma(X_t W_{xf} + H_{t-1} W_{hf} + b_f) \tag{15}$$

$$O_t = \sigma(X_t W_{xo} + H_{t-1} W_{ho} + b_o) \tag{16}$$

Where $W_{xi}, W_{xf}, W_{xo} \in R^{d\times h}$ and $W_{hi}, W_{hf}, W_{ho} \in R^{h\times h}$ are weight parameters and $b_i, b_f, b_o \in R^{1\times h}$ is deviation parameter. Next, the candidate memory cell $\tilde{C}_t$ is calculated. It uses the tanh function in the range [-1,1] as the activation function. The calculation formula is as follows:

$$\tilde{C}_t = tanh(X_t W_{xc} + H_{t-1} W_{hc} + b_c)$$

$$tanhx = \frac{sinhx}{coshx} = \frac{e^x - e^{-x}}{e^x + e^{-x}}$$

where $W_{xc} \in R^{d\times h}$ and $W_{hc} \in R^{h\times h}$ are weight parameters and $b_c \in R^{1\times h}$ is deviation parameter. Next, the memory cell C_t state of the current time step is calculated. LSTM controls the flow of information in the hidden state through input gates, forget gates, and output gates, and this is also generally achieved using of multiplication by element. It can be seen from Fig. 5 that the calculation of current time step memory cell $C_t \in R^{n\times h}$ combines the information of previous time step memory cell and current time step candidate memory cell and controls the flow of information through forgetting gate and input gate. The calculation formula is as follows[39]:

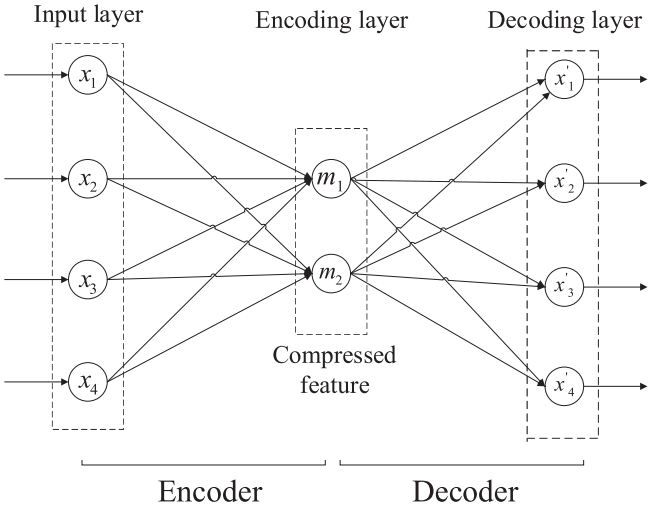

Fig. 6. The structure of autoencoder.

$$C_t = F_t \odot C_{t-1} + I_t \odot \tilde{C}_t \tag{19}$$

With the memory cell state, we can control the information flow from the memory cell to the hidden state $H_t \in R^{n\times h}$ through the output gate

$$H_t = O_t \odot tanh(C_t) \tag{20}$$

After the calculation of the above steps, the final output calculation formula of the system is as follows:

$$y_t = W_{ym} H_t + b_y \tag{21}$$

2.4. Autoencoder

Autoencoder is an unsupervised neural network model. It can learn the implicit characteristics of the input data, which is called encoding. At the same time, the original input data can be reconstructed with the learned new features, which is called decoding [25]. The autoencoder is a neural network with a three-layer structure of input layer, coding layer and decoding layer. It can be used as a feature extractor. The input layer and decoding layer contain the same number of nodes and both are larger than the corresponding number of nodes in the encoding layer. The network structure of the automatic encoder is shown in Fig. 6

The encoding layer of the automatic encoder tries to express the

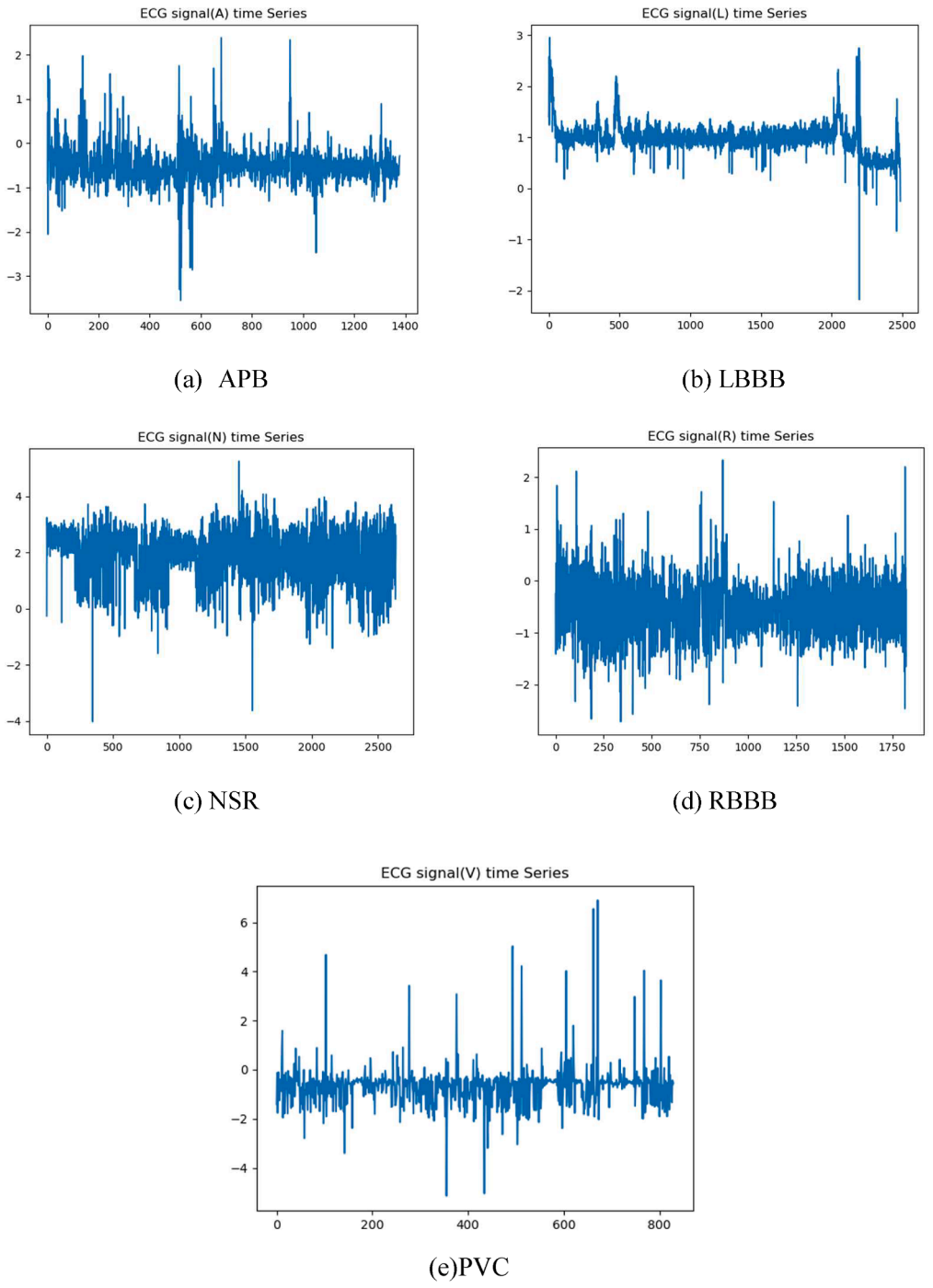

Fig. 7. The time series of five heartbeat types in lead MLII lead:(a)APB,(b)LBBB,(c)NSR,(d)RBBB,(e)PVC.

input data sequence with low dimensional data sequence m. The output formula of coding layer is as follows:

$$m = f(Wx + b) \tag{22}$$

where f is the activation function. W is the weight matrix and b is the deviation vector. Then, in the decoding layer of the automatic encoder, m is mapped to the reconstructed data sequence $x^{'}$:

$$x^{'} = f^{'}(W^{'}m + b^{'}) \tag{23}$$

$f^{'}$, $W^{'}$ and $b^{'}$ in formula (23) are the corresponding terms of f, W and b in formula (22). We use Mean Absolute Error (MAE) as a loss function to measure the reconstruction error of the autoencoder. The formula is as follows [40]:

$$L(x - x^{'}) = \frac{\sum_{n=1}^{n} \left| x_i^{'} - x_i \right|}{n} \tag{24}$$

From an intuitive point of view, autoencoders can be used for feature dimensionality reduction, similar to PCA, but its performance is stronger than PCA, because the neural network model can extract more effective new features [26]. In addition to feature dimensionality reduction, the new features learned by the autoencoder can be fed into the supervised learning model, so the autoencoder can function as a feature extractor.

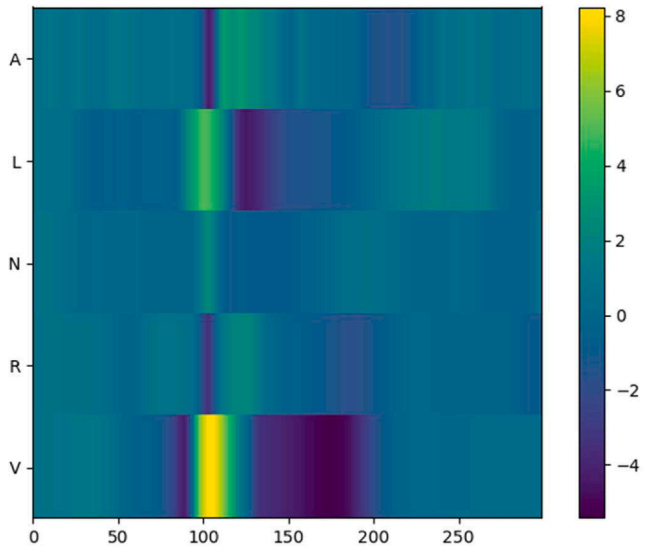

Fig. 8. Visual diagram of single beat heartbeat of five heartbeat types.

2.5. Time series

A time series is a set of random variables ordered in time. It is usually the result of observing a potential process at a given sampling rate in an equally spaced time period [27]. Time series data essentially reflects the changing trend of one or some random variables with time. The core of the time series forecasting method is to dig out this law from the data and use it to make an estimate of the future data. Therefore, time series analysis is based on the continuous law of the development of objective things, using historical data in the past, and further inferring the future development trend through statistical analysis.

As a kind of continuous and repetitive special signal, the time series of ECG is very important. The respective time series of five different types of ECG signals collected above are shown in Fig. 7:

From Fig. 7, the time series of five different types of ECG signals are different in magnitude and frequency. We divided five different types of continuous ECG signals into single heartbeat beats. Each single beat heartbeat consists of 300 sampling points. Then calculate the average value of the signal amplitude of these single heartbeat beats at the same time acquisition point to form the representative value of each single heartbeat beat. Visualize the single beat of these five heartbeats, as shown in Fig. 8.

Among them, A, L, N, R and V on the longitudinal axis represent five different types of heartbeat: atrial premature beats (APB), left bundle branch block (LBBB), normal heartbeat (NSR), right bundle branch block (RBBB) and ventricular premature beats (PVC). The row corresponding to each heartbeat on the vertical axis represents the time series of that heartbeat. From the figure, we can clearly understand that different types of ECG signals have their own unique time series distribution. The classification model we designed this time relies on extracting these time series features hidden in ECG signals for classification.

2.6. The architecture

In order to effectively learn the time series characteristics of ECG signals, we propose a new automatic encoder based on LSTM. In the network structure of the model, the input layer includes a channel. After the input layer is the coding layer of the automatic encoder. The coding layer is mainly composed of three layers of LSTM network, and its structure is shown in Fig. 8. The input data of the LSTM neural network layer of the first layer is the transformation tensor of the original ECG signal data input, in which the dimension of the hidden layer is set to 256. The input data of the second layer LSTM neural network layer is the transformation tensor of the output of the first layer LSTM layer, and the dimension of the hidden layer is set to 128. The input data of the third layer LSTM neural network layer is the transformation tensor of the output of the second layer LSTM neural network layer, and the dimension of the hidden layer is set to 64. Finally, the forward function is defined to make the original ECG signal data output sequentially through the three-layer LSTM neural network layer. The multifold reduced hidden layer is used to compress the original data and extract the time series information hidden in the data through LSTM.

After the encoding layer is the decoding layer of the autoencoder. The decoding layer is mainly composed of a three-layer LSTM network and a linear layer connected step by step, and its structure is shown in Fig. 9. The dimension of the hidden layer of the first layer LSTM neural network layer is set to 64. The input data of the second layer LSTM

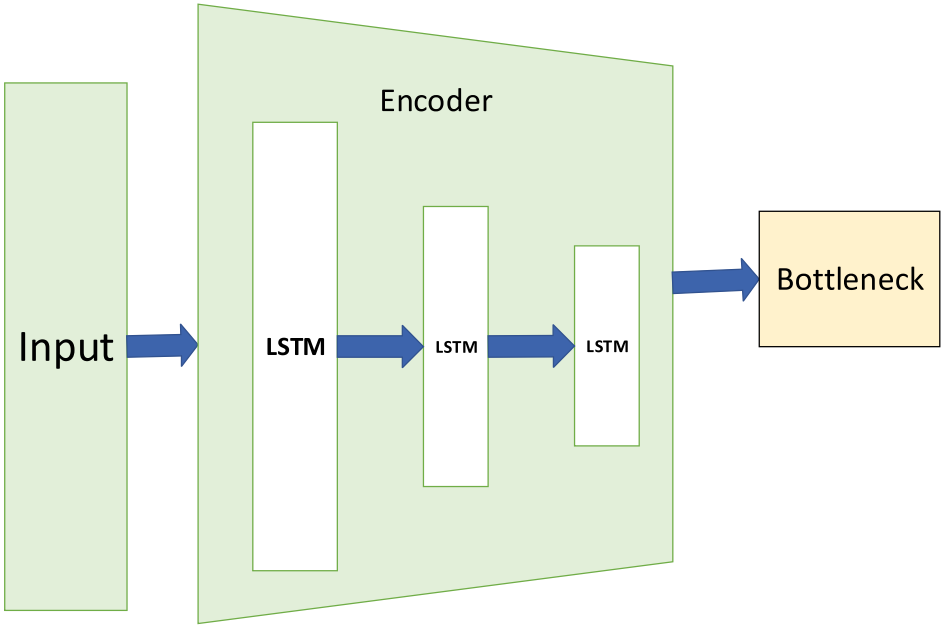

Fig. 9. Encoder layer structure diagram.

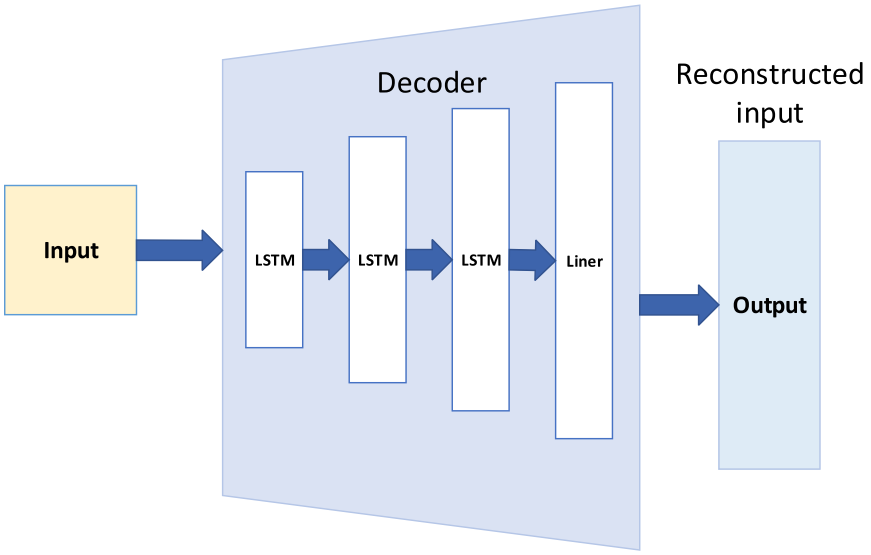

Fig. 10. Decoder layer structure diagram.

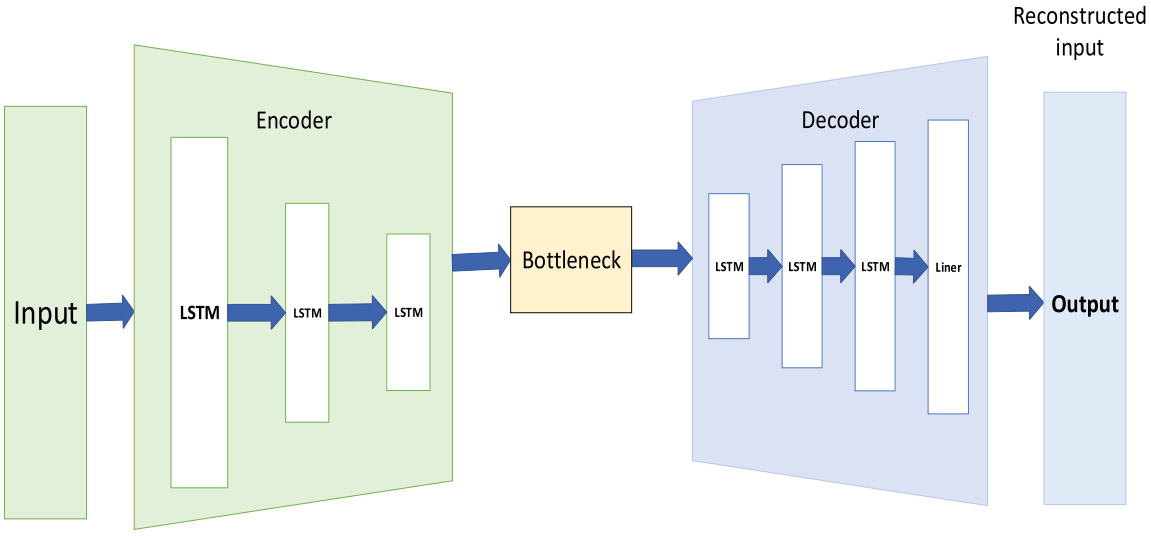

Fig. 11. Overall structure diagram of autoencoder.

Table 3
Details and parameters of each layer of autoencoder based on LSTM.

No	Layer Name	Unit Size	Other Layer Parameters
1	LSTM	256	Return Sequences = True
2	LSTM	128	Return Sequences = True
3	LSTM	64	Return Sequences = True
4	LSTM	64	Return Sequences = True
5	LSTM	128	Return Sequences = True
6	LSTM	256	Return Sequences = True
7	Liner	256*300	

neural network layer is the transformation tensor of the output of the first layer LSTM layer, and the dimension of the hidden layer is set to 128. The input data of the third layer LSTM neural network layer is the conversion tensor of the output of the second layer LSTM neural network layer, and the dimension of the hidden layer is set to 256. Finally, the linear layer is used to transform the output tensor format into the standard input ECG data format, and the multiplied hidden layer is used to reconstruct and output the compressed data sequence in the coding layer, which can save the time series characteristics of the processed data. The overall structure of the autoencoder is shown in Fig. 10.

The details of the parameters of each layer of the automatic encoder are shown in Table 3. Because time series is a group of random variables sorted by time. It is the result of observing a potential process at a given sampling rate in equal intervals. Therefore, in order to obtain the time series characteristics hidden in the ECG data sequence, a group of single heartbeat beat data sequence is input into the above autoencoder model. The LSTM network layer of layer 1–3 in Table 3 compresses the input single heartbeat beat data layer by layer from the size of 1 * 300 to the size of 1 * 64. It is used to extract and learn the time series characteristics of single heartbeat beat data series. Then, the compressed data is re expanded to 1 * 300 size through layer 4–7 LSTM network layer and linear layer in Table 3. Then, the error between the expanded data and the original data is calculated, and then the back-propagation method is used to update the parameters in the model. As an unsupervised learning algorithm, the designed autoencoder classification model finally obtains the time series characteristics of the same ECG type data by continuously iterating the above process. The specific validation experiments are as follows. We used the above new LSTM automatic encoder to train five

Table 4
Confusion matrix obtained by applying classification model on MIT-BIH arrhythmia database.

		Predicted					Acc(%)	Se(%)	+P(%)
		A	L	N	R	V			
Original	A	252	1	8	0	1	98.57	95.09	96.18
	L	5	677	14	4	0		98.54	96.71
	N	5	5	6279	6	5		99.34	99.66
	R	2	3	10	615	1		98.08	97.46
	V	1	1	10	2	607		98.85	97.74

Acc: accuracy, Se: Sensitivity, +P: Positive predictivity.

different types of ECG training data sets to extract the time series features of their heartbeat types. The same ECG signal is the output after experiencing the encoding and decoding of the autoencoder, and then the reconstruction error is calculated based on this input. Equation (24) is used to calculate the error. Then the internal parameters of the model are updated continuously through forward feedback and back propagation to make the error between the reconstructed output and the original input smaller and smaller. In other words, we can better learn the time series characteristics of each heartbeat type. Finally, the error between the output data sequence and the input data sequence becomes stable, and the model training and the collection of the time sequence characteristics of various types of ECG signals are completed. The result is shown in Fig. 12.Fig. 13

Fig. 11 (a) shows the error values and distribution of the output sequence and input sequence of APB type ECG signals after they pass through an autoencoder with characteristic parameters of APB type time series. Fig. 11 (b) shows the error values and distribution of the output sequence and input sequence of non-APB type ECG signals after they pass through an autoencoder with characteristic parameters of APB type time series. Fig. 11 (c) shows the error values and distribution of the output sequence and input sequence of LBBB type ECG signals after they passed through the autoencoder with characteristic parameters of LBBB type time series. Fig. 11 (d) is the error value and distribution diagram of the output sequence and input sequence of non-LBBB type ECG signals after they passed through an autoencoder with characteristic parameters of LBBB type time series. Fig. 11 (e) is the error value and distribution diagram of the output sequence and input sequence of NSR type ECG signals after they passed through the autoencoder with characteristic parameters of NSR type time series. Fig. 11 (f) is the error value and distribution diagram of the output sequence and input sequence of non-NSR type ECG signals after they passed through the autoencoder with characteristic parameters of NSR type time series. Fig. 11 (g) is the error value and distribution diagram of the output sequence and input sequence of RBBB type ECG signals after they passed through an autoencoder with characteristic parameters of RBBB type time series. Fig. 11 (h) is the error value and distribution diagram of the output sequence and input sequence of non-RBBB type ECG signals after they pass through an autoencoder with characteristic parameters of RBBB type time series. Fig. 11 (I) shows the error values and distribution of the output sequence and input sequence of PVC type ECG signals after they passed through the autoencoder with characteristic parameters of PVC type time series. Fig. 11 (j) is the error value and distribution diagram of the output sequence and input sequence of non-PVC type ECG signals after they passed through the autoencoder with characteristic parameters of PVC type time series.

Taking (a) and (b) in Fig. 11 as examples, it can be clearly seen that when APB-type ECG signals pass through the autoencoder that has learned the characteristics of APB-type heartbeat time series, the error value of reconstructed signals is basically below 0.1. However, the error values of other ECG signals of any type are basically distributed above 10 after the reconstruction by the same autoencoder. Therefore, we can conclude that APB type heartbeat can be distinguished from other types of heartbeat by the new LSTM autoencoder. The other four heartbeat types can also be distinguished by the LSTM autoencoder. So we can get the final heartbeat classification model, the model structure is shown in Fig. 12.

When the data of a heartbeat beat signal is input into the model in Fig. 12, five LSTM autoencoders with different types of ECG signal time series characteristics are respectively fed into them, and then the types of input ECG signals are judged according to the errors of reconstructed signals of five different LSTM autoencoders. The heartbeat type of the autoencoder with the smallest reconstruction error corresponds to the type of the input heartbeat. The class based feature visualization obtained by the classification model is shown in Fig. 14.

It can be seen from Fig. 14 that the classification model we designed can extract useful time series features in different kinds of ECG signals as the classification basis.

3. Results

This work was running on the deep learning framework of pytorch. The workstation used consists of 8 GB GPU (NVIDIA GeForce GTX-1070), Intel i7-4790 processor (3.60 GHz) and 8 GB RAM. 46/5000 We also designed autoencoders of the same principle composed of different numbers of LSTM network layers for comparative experiments, as shown in Table 5. We proposed an autoencoder with two LSTM network layers in both encoding layer and decoding layer, an autoencoder with four LSTM network layers in both encoding layer and decoding layer, and an autoencoder with eight LSTM network layers in both encoding layer and decoding layer. Five validation data sets of ECG signals which were not used during training were brought into the model to verify the completion of the model task. Accuracy, precision, and recall are used to evaluate the classification performance of the model. The calculation formula of these standards is as follows:

$$Accuracy = \frac{TP + TN}{TP + TN + FP + FN} \tag{25}$$

$$\text{Precision} = \frac{TP}{TP + FP} \tag{26}$$

$$Sensitivity = \text{Recall} = \frac{TP}{TP + FN} \tag{27}$$

Among them, *TP* is true positive, *FP* is false positive, *TN* is true negative and *FN* is false negative. The encoder layer and decoder layer of the autoencoder model in this design are composed of three LSTM network layers. The classification model is tested on MIT-BIH arrhythmia database and MIT-BIH supraventricular arrhythmia database respectively. The confusion matrices obtained are shown in Table 4 and Table 5 respectively.

It can be shown from Table 4 that the accuracy rate of the classification model we designed this time could reach 98.31% in MIT-BIH arrhythmia database and 97.59% in MIT-BIH supraventricular arrhythmia database. From the information comparison in Table 5, it can be shown that when the number of LSTM layers of encoding layer and decoding layer is less than 3, although the processing speed became faster, the accuracy of the model decreased. When the number of layers is more than 3, the accuracy of the system was not significantly improved, but the processing time was greatly increased, which is not

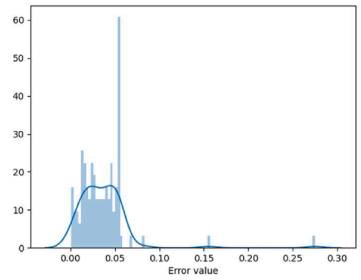

(a)ABP+ABP autoencoder error distribution

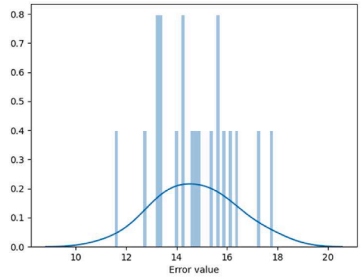

(b)Other+ABP autoencoder error distribution

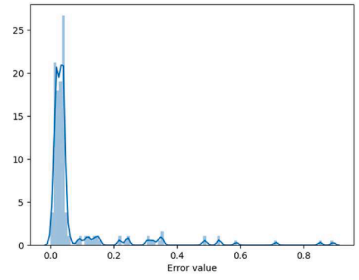

(c)LBBB+LBBB autoencoder error distribution

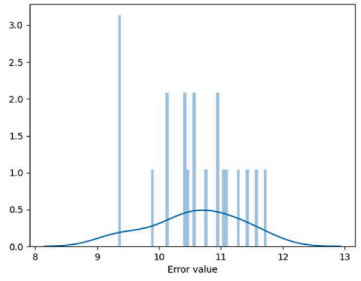

(d)Other+LBBB autoencoder error distribution

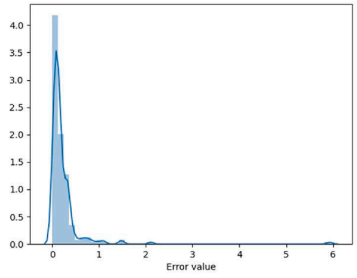

(e)NSR + NSR autoencoder error distribution

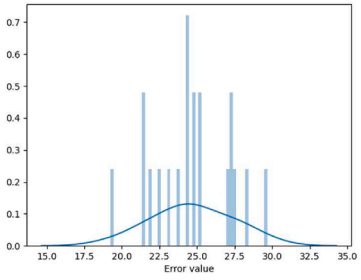

(f)Other+ NSR autoencoder error distribution

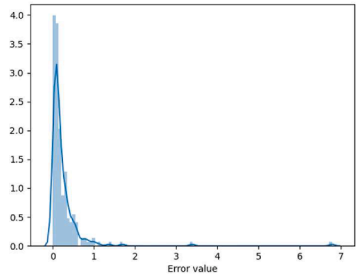

(g)RBBB+RBBB autoencoder error distribution

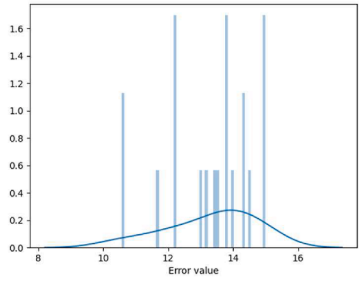

(h)Other +RBBB autoencoder error distribution

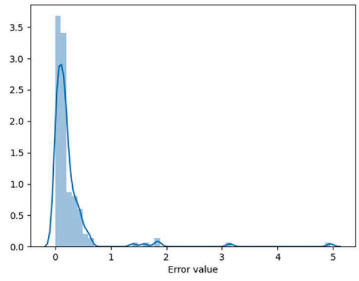

(i)PVC+PVC autoencoder error distribution

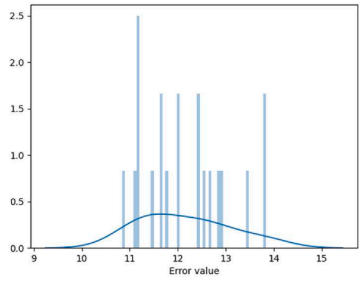

(j)Other+PVC autoencoder error distribution

Fig. 12. The output and input error distribution of five different types of heartbeat through the corresponding time series and non-corresponding time series autoencoder respectively.

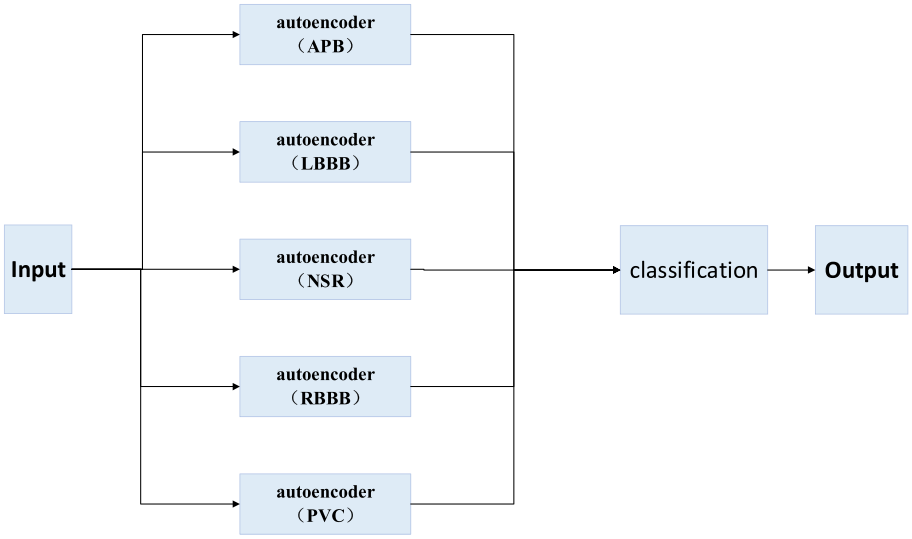

Fig. 13. Overall flow chart of heartbeat classification.

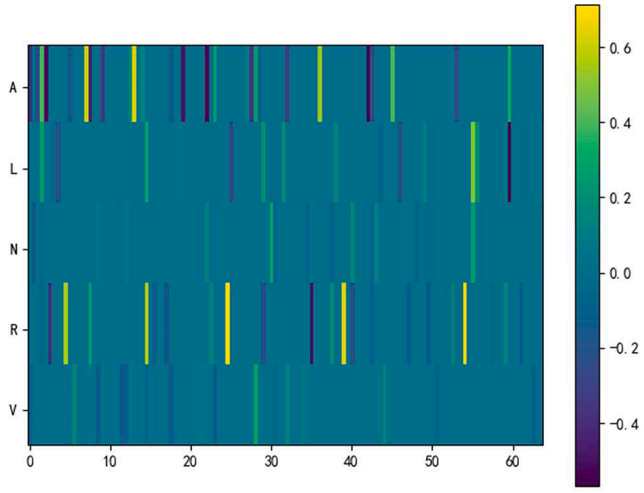

Fig. 14. Class based feature visualization obtained from the model.

suitable for use. Therefore, we can draw a conclusion that the optimal number of LSTM network layers to constitute this heartbeat classification model is 3.

4. Discussion

In recent years, MIT-BIH arrhythmia database has become a hot topic in arrhythmia classification research. Table 8 lists some classical methods and results proposed by previous researchers. Sahoo et al. [28] used wavelet transform based on multi-resolution to extract features and complete heartbeat classification and detection. Li et al. [29] used KICA and DWT to extract ECG features from time domain and frequency domain respectively and complete classification. Yeh et al. [30] extracted morphological features directly from ECG components, and then used them for heartbeat classification. Elhaj et al. [31] used a combination of neural networks and support vector machines to classify heartbeats and achieved very good experimental results. Martis et al. [32] performed beat segmentation of ECG signal, and then implemented principal component analysis to complete the classification of ECG signal.

Many deeping learning methods have also been proposed by researchers for classification detection of arrhythmias. Oh et al. [33] combined CNN and LSTM to diagnose arrhythmia. Acharya et al. [1] used CNN to identify and classify ECG signals and obtained a good accuracy. They also proposed another ECG signal detection and classification method in the same year [34]. There are other studies that have also obtained good experimental results [35–36]. In our study, it is shown in Table 4 that our proposed model achieveds 98.57% accuracy, 97.98% recall and 97.55% positive precision. In order to verify the practicability and stability of the model, we also extracted the ECG experimental data of the same specification from MIT-BIH supernatural arrhythmia database for verification. From Table 5, we can see that the accuracy of our proposed model is 97.59%, the recall rate is 93.91% and the precision is 94.52%.

In the design method proposed in this paper, the preprocessing process of ECG signal is also very important. For the single beat heartbeat of different types of ECG signals under the same time limit, the amplitudes of different types of heartbeat in the corresponding signal bands such as P wave, QRS complex and T wave are different. Professional doctors also judge different heartbeat types from this point of view. However, there are some types of heartbeats that do not differ significantly in amplitude within the same band. And in the process of collecting ECG signals, due to the skin polarization phenomenon and the

Table 5
Confusion matrix obtained by applying classification model on MIT-BIH supraventricular arrhythmia database.

		Predicted					Acc(%)	Se(%)	+P(%)
		A	L	N	R	V			
Original	A	240	5	5	8	4	97.59	89.55	91.60
	L	10	647	20	13	10		94.87	92.43
	N	7	18	6235	20	20		99.17	98.97
	R	5	4	4	613	5		92.32	97.15
	V	6	8	23	10	574		93.64	92.43

Acc: accuracy, Se: Sensitivity, +P: Positive predictivity.

Table 6
Performance detail table of LSTM autoencoder with different network layers.

Models	Time Cost	Classification Accuracy	
		Training	Testing
2-layer LSTM	12,600 sec (3.5 h)	94.77%	93.47%
3-layer LSTM	16,500 sec (4.5 h)	98.31%	98.57%
4-layer LSTM	21,600 sec (6 h)	97.64%	98.11%
8-layer LSTM	29,880 sec (8.3 h)	98.28%	97.13%

problems of the acquisition equipment itself, power frequency interference and other interference signals inevitably exist in the collected signals. It makes it more difficult to distinguish the parts with small amplitude difference between some heartbeats. The classification model can not collect effective time series classification features. In order to improve the accuracy of classification methods, we designed a preprocessing process. In order to confirm this conclusion, we also use the same classification model to experiment on the unprocessed ECG data. The confusion matrix results are shown in Table 7.

In addition, some recent studies on ECG classification are listed in Table 9. It is briefly compared with our classification model. Gómez et al. Constructed an ECG classification model using bidirectional Long Short-Term Memory (LSTM) network, which includes 5-layer LSTM network. The final accuracy is 82.10%. Tang et al. Completed the task of ECG classification by using LSTM network and ECG morphological features. The accuracy of the model is 82.14%. Obviously, compared with the above two models, the model we designed has higher accuracy. Compared with the design method of five layer LSTM network directly given by Gómez et al., we conduct comparative experiments by designing classification models composed of different number of LSTM network layers. The experimental results are shown in Table 6. Finally, the optimal classification model is found under the requirements of less time-consuming model training and high accuracy, so our design is more convincing. Compared with the method of Tang et al., our classification model does not need to manually set the calculation of morphological features such as RR interval in advance. Hammad et al. Used deep neural network and genetic algorithm to complete the task of feature extraction and classification of ECG signals. Chen et al. Used an arrhythmia detection model based on the fusion of CNN and BLSTM. The morphological information of the current heartbeat beat and the time information of adjacent heartbeat beats are collected as the judgment basis of heartbeat classification. Wang et al. Used CNN to adopt the methods of multi-scale feature extraction and cross-scale information complementarity for ECG signals, obtained multiple convolution kernels in different acceptance domains, and realized the feature extraction of signal segments of different sizes. Their methods have achieved good results. However, when the network level of CNN is too deep, the parameters near the model input layer will change slowly by using BP propagation to modify the parameters. The problems of gradient disappearance and gradient explosion can not be avoided. And some methods also need to manually set the feature extraction interval in advance. But obviously, a

Table 8
Studies on the automated detection of the arrhythmias.

Author, Year	#of beats	Approach	Performance
Sahoo et al., 2017[28]	109,494	DWT, SVM	Acc:98.39% Se:99.87% +P:99.21%
Li et al., 2016[29]	1800	DWT, kernel ICA and PCA, SVM	Acc: 98.8% Se: 98.50% +P:98.91%
Yeh et al., 2009[30]	102,060	Linear, Discriminant, Analysis	Acc: 96.23% Se: 92.49%
Elhaj et al., 2016[31]	110,094	DWT, PCA, HOS, ICA, SVM-RBF	Acc: 98.91% Se: 98.91%
Martis et al., 2011[32]	1247	Support Vector Machine (Radial Basis Function)	Acc: 98.48% Se: 98.90%
Oh et al., 2018[33]	16,499	LSTM and CNN	Acc: 98.10% Se: 97.50% +P:98.69%
Acharya et al., 2017 [1]	109,449	CNN	Acc: 94.03% Se: 96.71%
Acharya et al., 2017 [34]	21,709	CNN	Acc: 92.50% Se: 98.09%
Zubair et al., 2016 [35]	100,389	CNN	Acc: 92.70%
Kiranyaz et al., 2016 [36]	83,648	CNN	Acc: 99.00% Se: 93.90%
This study	97,300	LSTM, Autoencoder	Acc: 98.57% Se: 97.98% +P:97.55%

Acc: accuracy, Se: Sensitivity, +P: Positive predictivity; CNN: Convolutional Neural Network; LSTM: Long Short-Term Memory; DWT: Discrete wavelet transform; SVM-RBF: Support V ector Machine (Radial Basis Function); ICA: Independent Component Analysis; PCA: Principal.
Component Analysis; HOS: High Order Statistics.

Table 9
Table of recent research information.

Author, Year	Classifier	Database	#of classes	Performance
Gómez et al., 2021[41]	LSTM	MIT-BIH	2	Acc: 82.10% Se: 78.40% +P:84.79%
Tang et al., 2021[42]	LSTM, Morphological features	MIT-BIH	2	Acc: 82.14% Se: 87.14% +P:79.22%
Chen et al., 2020[44]	CNN, BLSTM	MIT-BIH	4	Acc: 96.77% Se: 74.89% +P:81.24%
Hammad et al., 2020 [45]	DNN	MIT-BIH	5	Acc: 98.00% Se: 99.70% +P:95.80%
Wang et al., 2020[46]	CNN	CPSC_2018, PhysioNet/ CinC_2017	9, 4	Acc: 82.80% Se: 82.20%
This study	LSTM, Autoencoder	MIT-BIH SVDB	5, 5	Acc: 98.57% Se: 97.98% +P:97.55%

Table 7
ECG classification confusion matrix without preprocessing.

		Predicted					Acc(%)	Se(%)	+P(%)
		A	L	N	R	V			
Original	A	171	26	28	23	14	90.83	61.96	65.27
	L	32	517	98	32	21		75.36	73.86
	N	58	121	5932	129	60		96.75	94.16
	R	7	8	20	581	15		74.58	92.08
	V	8	14	53	14	532		82.87	85.67

Acc: accuracy, Se: Sensitivity, +P: Positive predictivity.

large number of feature extraction will bring a great burden. Our method only needs the ECG signal to be input into the model for training and verification through the simple filtering preprocessing process designed by us.

5. Conclusions

Early diagnosis of arrhythmia types is of great importance in reducing the risk and incidence rate of cardiovascular events. In the arrhythmia classification research carried out in recent years, a considerable number of researchers only give the structural details such as the number of network design layers when using LSTM network to design ECG classification model, and do not explain the design reasons too much. This time, we designed and optimized the classification model based on LSTM network, and found the optimal structure of the optimized classification algorithm by comparative experiment. This paper designs and optimizes a new network layer design based on LSTM, and obtains the autoencoder classification model. The advantages of this model are:

a. There is no need to manually set the model input parameters in advance, and the preprocessed ECG signals can be trained and classified directly.
b. This method discards the serious problem of gradient disappearance in the ECG classification model composed of traditional convolutional neural network. It has good stability.
c. Compared with other complex ECG classification models based on deep learning algorithm, this model has the same or even higher accuracy, but the structure and principle of the model are relatively simple and easy to understand.
d. Through comparative experiments, it is confirmed that the design method has achieved the optimal effect in the research of the same type of methods.

Of course, the classification model of this design also has disadvantages. The ECG classification method designed in this paper mainly uses the judgment feature of ECG time series. If we can comprehensively consider the effective judgment features proposed in other previous studies (such as wavelet transform, ECG morphological features, etc.), the model results will be more reliable. In future studies, we will try to combine more deep learning methods to improve the classification performance of arrhythmia heartbeat.

CRediT authorship contribution statement

Pengfei Liu: Conceptualization, Methodology, Software, Investigation, Writing – review & editing. **Xiaoming Sun:** Conceptualization, Methodology, Supervision. **Yang Han:** Writing – original draft, Visualization. **Zhishuai He:** Software, Visualization. **Weifeng Zhang:** Validation, Formal analysis. **Chenxu Wu:** Software, Data curation.

Declaration of Competing Interest

The authors declare that they have no known competing financial interests or personal relationships that could have appeared to influence the work reported in this paper.

Acknowledgement

This research was supported by the Fundamental Research Funds for the Universities in Heilongjiang Province (2018-KYYWF-1681), the University Nursing Program for Young Scholars with Creative Talents in Heilongjiang Province (UNPYSCT-2017086), and National Natural Science Foundation of China (61671190, 61571168).

References

[1] U.R. Acharya, S.L. Oh, Y. Hagiwara, J.H. Tan, M. Adam, A. Gertych, R.S. Tan, A deep convolutional neural network model to classify heartbeats, Comput. Biol. Med. 89 (2017) 389–396.
[2] C. LIN, Y. DU, T. CHEN, Adaptive wavelet network for multiple cardiac arrhythmias recognition, Expert Syst. Appl. 34 (4) (2008) 2601–2611.
[3] Michel Misiti, Yves Misiti, Georges Oppenheim, Jean-Michel Poggi, Wavelet Toolbox for use with MATLAB, vol. 1, March 1996.
[4] H.M. Rai, A. Trivedi, S. Shukla, ECG signal processing for abnormalities detection using multi-resolution wavelet transform and Artificial Neural Network classifier, Measurement 46 (9) (2013) 3238–3246.
[5] Rajpurkar P , Hannun A Y , Haghpanahi M, et al. Cardiologist-Level Arrhythmia Detection with Convolutional Neural Networks. 2017.Rajpurkar P , Hannun A Y , Haghpanahi M , et al. Cardiologist-Level Arrhythmia Detection with Convolutional Neural Networks. 2017.
[6] U.R. Acharya, H. Fujita, S.L. Oh, U. Raghavendra, J.H. Tan, M. Adam, A. Gertych, Y. Hagiwara, Automated identification of shockable and non-shockable life-threatening ventricular arrhythmias using convolutional neural network, Future Generation Computer Systems 79 (3) (2018) 952–959.
[7] N. Srinivasan, D.F. Ge, S.M. Krishnan, "Autoregressive modeling and classification of cardiac arrhythmias", in Proceedings of the Second Joint Conference Houston, TX, USA, October 2326, 2002.
[8] Risk, Marcel0 R and Sobh, Jamil F and Saul, J Philip, "Beat detection and classification of ECG using self organizing maps", Engineering in Medicine and Biology Society, 1997. Proceedings of the 19th Annual International Conference of the IEEE, vol 1, pp. 89-91, IEEE, Chicago, IL. USA.
[9] P. Malhotra, L. Vig, G. Shroff, P. Agarwal, Long Short Term Memory Networks for Anomaly Detection in Time Series, in: European Symposium on Artificial Neural Networks, vol 23, Computational Intelligence and Machine Learning, Belgium, 2015.
[10] T. Rui, S. Zhang, T. Ren, et al., Data Reconstruction Based on Supervised Deep Auto-Encoder[C]// Pacific Rim Conference on Multimedia, Springer, Cham, 2017.
[11] Y. Bengio, P. Simard, P. Frasconi, Learning long-term dependencies with gradient descent is difficult, IEEE Trans. Neural Networks 5 (2) (1994) 157–166.
[12] He K, Zhang X, Ren S, et al. Delving Deep into Rectifiers: Surpassing Human-Level Performance on ImageNet Classification. 2015.
[13] Saxe A M, Mcclelland J L, Ganguli S. Exact solutions to the nonlinear dynamics of learning in deep linear neural networks. 2013.
[14] G.B. Moody, R.G. Mark, The impact of the MIT-BIH Arrhythmia Database, IEEE Eng in Med and Biol 20 (3) (2001), 45–50 (May-June (PMID: 11446209).
[15] S. Chen, W. Hua, Z. Li, J. Li, X. Gao, Heartbeat classification using projected and dynamic features of ECG signal, Biomed. Signal Process. Control 31 (2017) 165–173.
[16] Braunwald E. (Editor), Heart Disease,"A Textbook of Cardiovascular Medicine", Fifth Edition, p. 108, Philadelphia, W.B. Saunders Co., 1997. ISBN 0-7216-5666-8.
[17] E.J.d.S. Luz, W.R. Schwartz, G. Cámara-Chávez, D. Menotti, ECG-based heartbeat classification for arrhythmia detection: A survey, Comput. Methods Programs Biomed. 127 (2016) 144–164.
[18] Turnip M, Dharma A , Andrian, et al. Integration of FIR and Butterworth Algorithm for Real-Time Extraction of Recorded ECG Signals[M]. 2021.
[19] Apolloni B , Marinaro M , R Tagliaferri. [Lecture Notes in Computer Science] Neural Nets Volume 2859 || An Adaptive Learning Algorithm for ECG Noise and Baseline Drift Removal. 2003, 10.1007/b13826(Chapter 15):139-147.
[20] S. Osowski, T.H. Linh, ECG beat recognition using fuzzy hybrid neural network, IEEE Trans. Biomed. Eng. 48 (2001) 1265–1271.
[21] (2013) Laplace Transform. In: Gass S.I., Fu M.C. (eds) Encyclopedia of Operations Research and Management Science. Springer, Boston, MA. https://doi.org/10.1007/978-1-4419-1153-7_200378.
[22] (2007) Adaptive Filters. In: Digital Signal Processing with Field Programmable Gate Arrays. Signals and Communication Technology. Springer, Berlin, Heidelberg. https://doi.org/10.1007/978-3-540-72613-5_8.
[23] Alexander S.T. (1986) The Least Mean Squares (LMS) Algorithm. In: Adaptive Signal Processing. Texts and Monographs in Computer Science. Springer, New York, NY. https://doi.org/10.1007/978-1-4612-4978-8_5.
[24] S. Hochreiter, J. Schmidhuber, Long short-term memory, Neural Comput. 9 (8) (1997) 1735–1780.
[25] Lempitsky V. (2020) Autoencoder. In: Ikeuchi K. (eds) Computer Vision. Springer, Cham. https://doi.org/10.1007/978-3-030-03243-2_862-1.
[26] Y.a. Song, G. Shi, L. Chen, X. Huang, T. Xia, Remaining useful life prediction of turbofan engine using hybrid model based on autoencoder and bidirectional long short-term memory, J. Shanghai Jiaotong Univ. (Sci.) 23 (S1) (2018) 85–94, https://doi.org/10.1007/s12204-018-2027-5.
[27] H.M. Yang, Z.S. Pan, W. Bai, Summary of time series prediction methods, computer science 46 (01) (2019) 21–28.
[28] S. Sahoo, B. Kanungo, S. Behera, S. Sabut, Multiresolution wavelet transform based feature extraction and ECG classification to detect cardiac abnormalities, Measurement 108 (2017) 55–66.
[29] H. Li, D. Yuan, Y. Wang, D. Cui, L.u. Cao, Arrhythmia classification based on multi-domain feature extraction for an ECG recognition system, Sensors 16 (10) (2016) 1744, https://doi.org/10.3390/s16101744.
[30] Y.-C. Yeh, W.-J. Wang, C.W. Chiou, Cardiac arrhythmia diagnosis method using linear discriminant analysis on ECG signals, Measurement 42 (5) (2009) 778–789.
[31] F.A. Elhaj, N. Salim, A.R. Harris, T.T. Swee, T. Ahmed, Arrhythmia recognition and classification using combined linear and nonlinear features of ECG signals. Comput. Methods Programs Biomed. 127 (2016) 52–63.

[32] R.J. Martis, U.R. Acharya, K.M. Mandana, A.K. Ray, C. Chakraborty, Application of principal component analysis to ECG signals for automated diagnosis of cardiac health, Expert Syst. Appl. 39 (14) (2012) 11792–11800.
[33] O.S. Lih E.Y.K. Ng T.R. San et al. Automated diagnosis of arrhythmia using combination of CNN and LSTM techniques with variable length heart beats. Computers in Biology and Medicine 2018:S0010482518301446-.
[34] U.R. Acharya, H. Fujita, O.S. Lih, Y. Hagiwara, J.H. Tan, M. Adam, Automated detection of arrhythmias using different intervals of tachycardia ECG segments with convolutional neural network, Inf. Sci. 405 (2017) 81–90.
[35] M. Zubair, J. Kim, C. Yoon, An automated ECG beat classification system using convolutional neural networks. 2016 6th International Conference on IT Convergence and Security (ICITCS), 2016.
[36] S. Kiranyaz, T. Ince, M. Gabbouj, Real-time patient-specific ECG classification by 1-D convolutional neural networks, IEEE Trans. Biomed. Eng. 63 (3) (2016) 664–675.
[37] X.-X. Yang, Y.-J. Xue, Design of a compact low-pass filter with wide stopband, J. Shanghai Univ. (Engl.) 12 (6) (2008) 495–497, https://doi.org/10.1007/s11741-008-0606-2.
[38] Faust, O., Acharya U, R., Krishnan, S. et al. Analysis of cardiac signals using spatial filling index and time-frequency domain. BioMed Eng OnLine 3, 30 (2004). https://doi.org/10.1186/1475-925X-3-30.
[39] J. Amin, M. Sharif, M. Raza, T. Saba, R. Sial, S.A. Shad, Brain tumor detection: a long short-term memory (LSTM)-based learning model, Neural Comput & Applic 32 (20) (2020) 15965–15973, https://doi.org/10.1007/s00521-019-04650-7.
[40] N. Tavakoli, S. Siami-Namini, M. Adl Khanghah, F. Mirza Soltani, A. Siami Namin, An autoencoder-based deep learning approach for clustering time series data, SN Appl. Sci. 2 (5) (2020), https://doi.org/10.1007/s42452-020-2584-8.
[41] Gómez J., Quispe A., Kemper G. (2021) A Comparative Study of Deep Learning Techniques Aimed at Detection of Arrhythmias from ECG Signals. In: Iano Y., Saotome O., Kemper G., Mendes de Seixas A.C., Gomes de Oliveira G. (eds) Proceedings of the 6th Brazilian Technology Symposium (BTSym'20). BTSym 2020. Smart Innovation, Systems and Technologies, vol 233. Springer, Cham. https://doi.org/10.1007/978-3-030-75680-2_43.
[42] Tang S., Tang J. (2021) c. In: Arabnia H.R., Deligiannidis L., Shouno H., Tinetti F. G., Tran QN. (eds) Advances in Computer Vision and Computational Biology. Transactions on Computational Science and Computational Intelligence. Springer, Cham. https://doi.org/10.1007/978-3-030-71051-4_67.
[43] S.D. Greenwald, Improved Detection And Classification Of Arrhythmias In Noise-Corrupted Electrocardiograms Using Contextual Information, Ph.D. thesis, Harvard-MIT Division of Health Sciences and Technology, 1990.
[44] A. Chen, F. Wang, W. Liu, S. Chang, H. Wang, J. He, Q. Huang, Multi-information fusion neural networks for arrhythmia automatic detection, Comput. Methods Programs Biomed. 193 (2020) 105479, https://doi.org/10.1016/j.cmpb.2020.105479.
[45] M.A. Hammad, A.M. Iliyasu, A. Subasi, et al., A multi-tier deep learning model for arrhythmia detection, IEEE Trans. Instrum. Meas. (2020) 99.
[46] R. Wang, J. Fan, Y. Li, Deep multi-scale fusion neural network for multi-class arrhythmia detection, IEEE J. Biomed. Health. Inf. (2020) 99, 1–1.
[47] G. Altan, Y. Kutlu, A.Özhan. Pekmezci, S. Nural, Deep learning with 3D-second order difference plot on respiratory sounds, Biomed. Signal Process. Control 45 (2018) 58–69.
[48] Altan G, Yayk A, Kutlu Y. Deep Learning with ConvNet Predicts Imagery Tasks Through EEG. Neural Processing Letters, 2021:1-16.Kiranyaz, S., T. Ince, and M. Gabbouj, Real-Time Patient-Specific ECG Classification by 1-D Convolutional Neural Networks. IEEE Transactions on Biomedical Engineering, 2016. 63 (3): p. 664-675.
[49] G. Altan, Y. Kutlu, N. Allahverdi, Deep learning on computerized analysis of chronic obstructive pulmonary disease, IEEE J. Biomed. Health. Inf. 24 (5) (2020) 1344–1350.
[50] G. Altan, Y. Kutlu, A. Gken, Chronic obstructive pulmonary disease severity analysis using deep learning on multi-channel lung sounds, Turkish J. Electric. Eng. Comput. Sci. 28 (5) (2020) 2979–2996.
[51] Altan G, Kutlu Y, Allahverdi N. A Multistage Deep Belief Networks Application on Arrhythmia Classification. 2016.
[52] G. Altan, Y. Kutlu, M. Yeniad, ECG based human identification using Second Order Difference Plots, Comput. Methods Programs Biomed. 170 (2019) 81–93.